Performance Analysis of Long Range Prediction for Fast Fading Channels[1]

Tugay Eyceoz, Shengquan Hu, and **Alexandra Duel-Hallen**
North Carolina State University
Dept. of Electrical and Computer Engineering
Center for Advanced Computing and Communication
Box 7914, Raleigh, NC 27695-7914
E-mail: {teyceoz, shu, sasha}@eos.ncsu.edu

Abstract – **Long range prediction capability for fading channels would provide enabling technology for accurate power control, reliable transmitter and/or receiver diversity, more effective adaptive modulation and coding and improvements in many other components of wireless systems. In order to achieve accurate long range prediction, the authors recently introduced a novel algorithm that finds the linear Minimum Mean Squared Error (MMSE) estimate of the future fading coefficient given a fixed number of previous observations. In this paper, we show that the superior performance of this algorithm is due to its lower sampling rate relative to the conventional (data rate) methods of fading estimation. We present the theoretical analysis of the MMSE of long range prediction as a function of several parameters: the number of scatterers, model order, sampling rate and the Signal-to-Noise ratio (SNR). Moreover, we show that the long range prediction can be further improved by employing adaptive tracking combined with the truncated channel inversion algorithm.**

1. INTRODUCTION

In wireless communication systems, signal fading due to multipath severely degrades performance and imposes high power requirements [1-3]. Since the channel changes rapidly, the transmitter and receiver are not generally optimized for current channel conditions, and thus fail to exploit the full potential of the wireless channel. Recently, several adaptive modulation and coding methods were proposed [4-8]. These techniques improve the bit rate for wireless channels by varying the transmitted signal according to current channel conditions. To realize the potential of adaptive transmission methods, the channel variations have to be reliably predicted several frames ahead. This prediction range is required due to the delay associated with the feed back of channel state information from the receiver to the transmitter, as well as processing delay and constraints on the rate of switching from one modulation format to another. In addition, reliable long-range prediction is necessary for adaptive transmitter diversity techniques, reliable power control and decision-directed channel estimation with delayed decisions. However, most current fading estimation techniques are not suitable for long-range prediction (e.g., [9,10].)

In [11-13], we described a novel long-range prediction algorithm that characterizes the channel as an autoregressive model (AR) with low sampling rate, and computes the MMSE estimate of the future fading coefficient sample based on a number of past observations. This algorithm can reliably predict future fading coefficients far beyond the coherence time for a flat fading channel with an arbitrary number of scatterers. The superior performance of this algorithm relative to conventional methods is due to its much lower sampling rate (on the order of twice the Doppler shift). For conventional techniques, the sampling rate is usually given by the date rate. The lower rate utilizes the large sidelobes of the autocorrelation function of the fading process, permitting prediction further into the future. In this paper, we analyze the potential of long-range prediction for fading channels and the performance of the algorithm proposed in [11-13]. We investigate the effect of the sampling rate, filter length, the number of scatterers and the SNR on the MMSE of long range prediction. We also discuss prediction in the presence of additive noise, and evaluate performance of prediction aided by adaptive tracking. It is shown that the potential of long range prediction for fading channels can be realized using properly chosen system parameters and adaptive tracking techniques.

2. LONG RANGE PREDICTION OF THE FADING CHANNEL

In this work, we concentrate on flat fading signals which result from interference between several coherent scattered components. The fading coefficient at the receiver is given by the sum of N Doppler shifted signals [1]

$$c(t) = \sum_{n=1}^{N} A_n e^{j(2\pi f_n t+\phi_n)} \qquad (1)$$

where (for the n^{th} scatterer) A_n is the amplitude, f_n is the Doppler frequency, and ϕ_n is the phase. Due to multiple scatterers, the fading signal varies rapidly for large vehicle speeds and undergoes "deep fades". Our approach to prediction of future fading conditions is based on the fact that the parameters A_n, f_n and ϕ_n vary much slower than the actual fading coefficient c(t).

Consider a binary phase shift keying (BPSK) discrete-time system model at the output of the matched filter and sampler:

$$y_k = c_k b_k + z_k \qquad (2)$$

where c_k is the fading signal c(t) sampled at the symbol rate, $E(|c_k|^2)=1$, b_k is the data sequence ($b_k \in \{+1,-1\}$), and z_k is the discrete complex AWGN process with variance $N_0/2$. Even for a modest number of scatterers, c(t) and c_k can be accurately modeled as correlated complex Gaussian random processes with Rayleigh distributed amplitudes and uniform phases [1-3], where the accuracy increases as N in (1) grows. This process is usually assumed to be stationary for purposes of describing short-term fading. However, the stationary Rayleigh fading process description does not reflect the variation of parameters associated with individual scatterers [14,15]. Similarly, in the popular deterministic Jakes model

[1] This research was supported by CACC (NC State University) and NSF grants CCR-9725271 and NCR-9726033

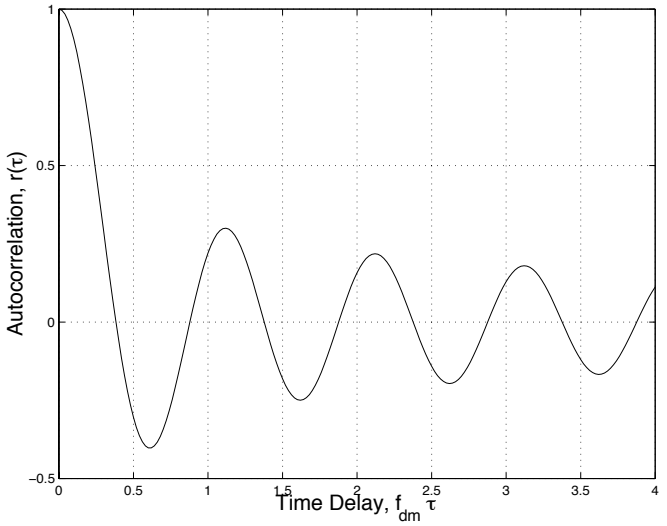

Figure 1. The theoretical autocorrelation function for the Rayleigh fading channel

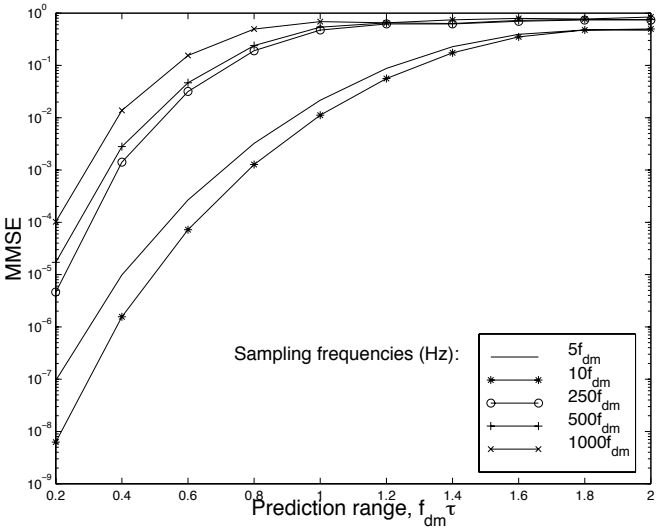

Figure 2. MMSE for long term prediction for different values of sampling rate, f_s, with the model order, p=20, and SNR = 140 dB.

[1], the amplitudes, frequencies and phases associated with the scatterers are fixed for the duration of the data frame. In [14,15] we show that the rate of parameter variation affects the accuracy of long range prediction. Therefore, it is important to take the time-variant nature of the channel into account in the analysis of this prediction method. However, in this paper, we use conventional stationary models to obtain computationally tractable estimates on the MMSE of long range prediction.

Our linear prediction (LP) method is based on the AR channel modeling [11]. We form the linear MMSE prediction of the future channel sample $\hat{c}_n$ based on p previously observed channel samples $c_{n-1}...c_{n-p}$:

$$\hat{c}_n = \sum_{j=1}^{p} d_j c_{n-j} \qquad (3)$$

where d_j's are the coefficients of the LP filter. Note that the samples have to be taken at least at the Nyquist rate given by twice the maximum Doppler frequency f_{dm} [1,2]. The sampling rate we choose is close to this Nyquist rate and therefore is much lower than the data rate in (2). The predicted samples are interpolated to forecast the fading signal at the data rate [11-13]. To date, most investigations of fading channel modeling and estimation assume sampling at the data rate (e.g., [9,10]). The low rate sampling is employed in pilot-symbol assisted techniques [16], although, to the extent our knowledge, it has not been applied for prediction prior to our work. Below, we show that the lower rate sampling results in much greater prediction accuracy when the filter length p in (3) is fixed, and evaluate the prediction MMSE as a function of prediction range, model order p and SNR for different sampling rates.

We start with the case when N in (1) is infinite (Rayleigh fading). The channel is modeled as the complex stationary Gaussian process with the autocorrelation function

$$r(\tau) = J_0(2\pi f_{dm}\tau) \qquad (4)$$

where $J_0(.)$ is the zero-order Bessel function of the first kind [1]. The plot of this function is shown in Figure 1. For illustration, let us fix the maximum Doppler frequency at 100Hz. Then the low sampling rate of 500Hz would correspond to 5 samples/unit of the x-axis of Fig. 1, whereas the data rate of 25KHz results in 250 samples/unit. When the model order p in (3) is fixed, the observation samples taken at the low sampling rate span much larger time interval than the samples at the data rate. This translates into exploitation of the sidelobes of the autocorrelation function in the prediction [17] and lower MMSE when low rate sampling is employed.

This observation can be quantified by considering a general channel prediction problem. For a given sampling rate $1/T_s$, the objective is to find the LP filter coefficients d_j which minimize the MSE, $E[|e(\tau)|^2]=E[|c(\tau) - \hat{c}(\tau)|^2]$, where τ is a prediction range, and $\hat{c}_\tau$ is an estimate of the future channel coefficient $c(\tau)$ given by the linear combination of p past samples $c_{-j}=c(-jT_s)$ (0 is the reference time, so the observations are taken for $t \le 0$):

$$\hat{c}(\tau) = \sum_{j=0}^{p-1} d_j c_{-j} \qquad (5)$$

Note that equation (3) applies prediction one sample ahead, whereas in (5) we compute the predicted value of the future sample separated from the observations by τ seconds. Thus, the coefficients d_j are not the same in (3) and (5) unless τ is the sampling interval. The optimal coefficients d_j are computed as

$$\underline{d} = \underline{R}^{-1}\,\underline{r} \qquad (6)$$

where $\underline{d} = (d_0 \cdots d_{p-1})$. $\underline{R}$ is the autocorrelation matrix (p×p) with coefficients $R_{ij} = E[c_{-i}\, c^*_{-j}]$ and $\underline{r}$ is the autocorrelation vector (p×1) with coefficients $r_j = E[c(\tau)\, c^*_{-j}]$. Note that when noisy observation are used in (5) (e.g. as in (2) with $b_k=1$), the effect of the noise is incorporated into $\underline{R}$ by adding $(N_0/2)\underline{I}$ where $\underline{I}$ is the p×p identity matrix, and r_j is modified to include noisy observations. The resulting minimum MSE is given by

$$E[|e(\tau)|^2] = 1 - \sum_{j=0}^{p-1} d_j r(\tau + jT_s) \qquad (7)$$

where $r(\tau)= E[c(t)c^*(t+\tau)]$ (see eq.(4) and Figure 1).

The MMSE performance of the long range prediction with various sampling rates is compared in Figure 2. A moderate model order, p=20, and a very high SNR = 140dB are chosen to illustrate the performance comparison, although, later, the results will be generalized for any p and SNR values. In this figure, the theoretical MMSE curves (7)

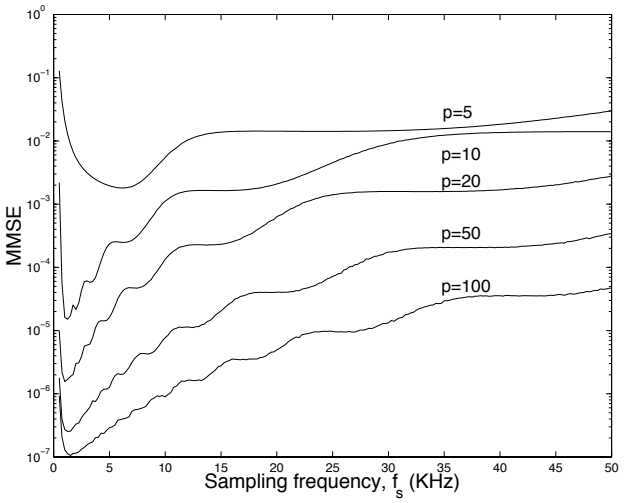

Figure 3. MMSE vs sampling rate, f_s, for various model orders p; prediction range τ = 4 ms, SNR=160dB and f_{dm}=100Hz.

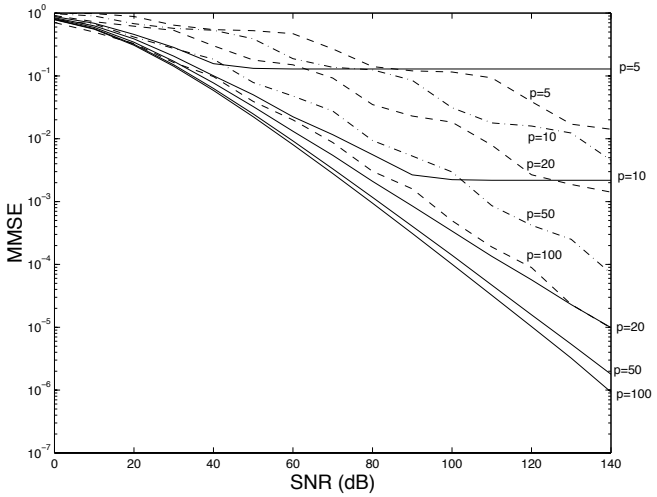

Figure 4. MMSE vs SNR for different values of model order, p, at data rate of 25 KHz (dashed lines) and f_s= 500 Hz (solid lines) for prediction range τ = 4 ms, f_{dm}=100Hz.

for a given prediction range are plotted. For example, assuming f_{dm}=100 Hz, the range of 0.2 on the x-axis corresponds to 50 data points ahead with the data rate of 25 kHz and 1 sampling point ahead with a lower sampling rate of 500 Hz. As seen from the figure, the same future value can be predicted with much greater accuracy by using the low sampling rates. Thus, when the sampling rate is reduced greatly relative to the data rate, but the filter length p remains the same, prediction much further ahead becomes feasible.

The effect of the sampling rate is explored further in Figure 3. In this figure, the MMSE vs f_s is plotted for various model orders, p, at the prediction range, $f_{dm}\tau$=0.4. As seen from the figure, for each model order there is an optimal low sampling rate that minimizes the MMSE. This optimal rate is close to 1KHz for moderate to high p. These results are obtained for an infinite number of scatterers, N. In this case, the lower sampling rate of 500 Hz is not the optimum rate. However, as we will see later in this paper, in the important practical case when the number of effective scatterers is modest [14,15], the MMSE decreases with the sampling rate for a fixed p, and the sampling rate of 500 Hz gives the best performance among the rates examined in Figure 3. Hence, we use f_s=500 Hz as a low sampling rate below to illustrate the performance of the MMSE with respect to SNR and p. In Figure 4, we demonstrate our MMSE results for different SNR values at the data rate of 25 KHz and at the low sampling rate of 500 Hz. Since the prediction range, $f_{dm}\tau$ = 0.4 is chosen for these curves, for the data rate of 25 KHz, 100 bits ahead are predicted. This range also corresponds to 2 low rate samples ahead. Since the sampling rate of 500 Hz is not the optimal rate for Rayleigh fading, for some values of SNR and p, high data rate might perform better. However, most of the time, the performance of the lower sampling rate is better than that of the high sampling rate. For lower sampling rates, we observe the saturation of the MMSE as the SNR increases. This MMSE floor can be found from (7) for a given value of p by setting N_0=0.

In Figure 5, the MMSE vs p is plotted in solid lines for $f_{dm}\tau$ = 0.2 and the sampling rate of $5f_{dm}$, for different values of SNR. As p increases the MMSE saturation level is approached. This MMSE floor corresponds to the prediction error given an infinite number of past observations for the fading process sampled at $5f_{dm}$ in the presence of noise. The closed form expression for this prediction error is given by

$$\text{MMSE}=\exp\left[\frac{1}{2\pi}\int_{-\pi}^{\pi}\log\frac{N_0}{P_x(w)+N_0}dw\right] \qquad (8)$$

where $P_x(w)$ is the folded power spectrum of the channel [2].

Given desired prediction range τ, the MMSE solution is found by solving for the filter taps in (6). However, in practice, this approach might be computationally expensive if several future samples have to be predicted at once. Instead, we use the one-step prediction at a given sampling rate (as in (3)) and then iterate equation (3) to predict more then one sample ahead by using previously predicted samples or their estimates when the observations are not available. Obviously, the MSE of this iterative prediction technique is lower bounded by (7).

So far, we investigated the case of the infinite number of scatterers in creating the Rayleigh fading environment. In Figure 6, the theoretical autocorrelation functions are plotted for the infinite number of oscillators, as well as for N=3 and 9. For the infinite number of oscillators, the autocorrelation function is given by (4), whereas for finite N, the autocorrelation function is found as [1]:

$$r(\tau)=\frac{4}{N_a}\sum_{n=1}^{N-1}\cos\left(2\pi f_{dm}\tau\cos\frac{2\pi n}{N_a}\right)+\frac{2}{N_a}\cos(2\pi f_{dm}\tau) \qquad (9)$$

where N_a= 4N-2. Note that the autocorrelation values for the finite values of N initially approximate the autocorrelation values of the Rayleigh fading. For large $f_{dm}\tau$, the autocorrelation functions diverge, and for finite N much larger sidelobes are present. These larger sidelobes help to reduce the MMSE as illustrated in Figure 7. In this Figure, the solid lines represent the MMSE curves using the theoretical autocorrelation functions for different N values. These theoretical MMSE values are closely approximated as the observation interval used to calculate the empirical autocorrelation values (and the resulting linear predictor coefficients) increases. Figure 7 depicts these simulation results for different number of oscillators and observation intervals. We have found that adaptive techniques can significantly improve prediction accuracy shown in Figure 7 for short observation intervals. The MMSE values in Figure 7 are high due to large additive noise in the observation. The

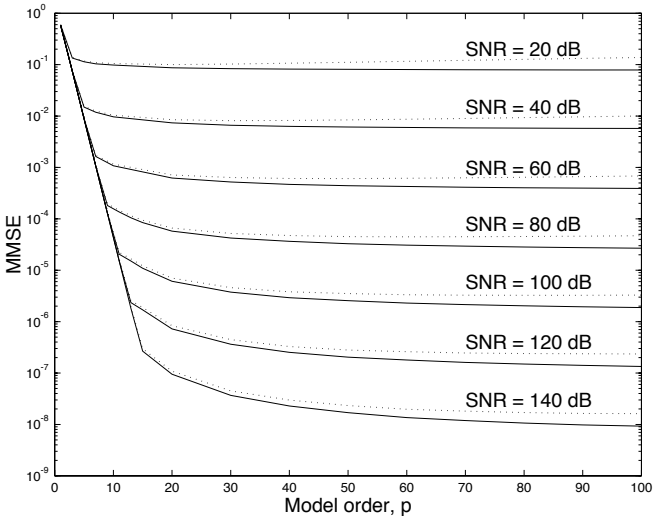

Figure 5. MMSE vs. model order, p, for different values of SNR for the sampling rate of 500 Hz, τ = 2ms, f_{dm}=100Hz. Solid lines: optimal approach; Dotted lines: adaptive tracking of linear prediction coefficients.

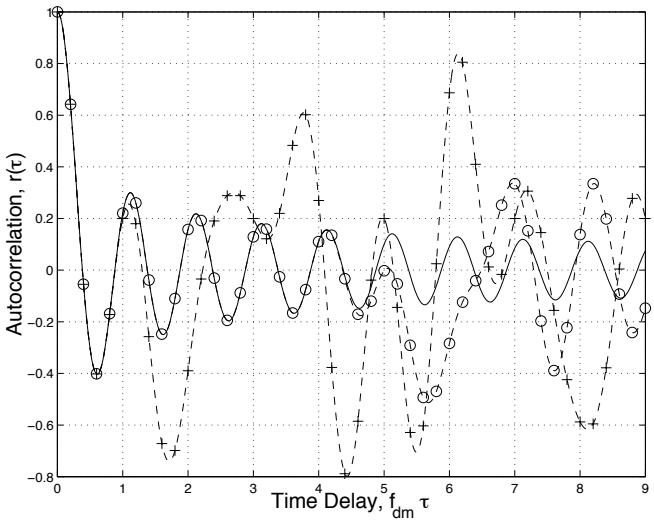

Figure 6. Theoretical autocorrelation functions for the infinite number of oscillators (Rayleigh fading) (solid line) and for a finite number of oscillators, N=3 (+ - - - +) and N=9 (o - - - o).

effect of the noise can be greatly reduced by using adaptive processing as shown in Section 3.

We mentioned earlier that the low sampling rate of 500 Hz (assuming f_{dm}=100Hz) does not result in the best performance for the infinite number of oscillators. However, when the number of oscillators is modest [14,15], the sampling rate of 500 Hz results in the smallest MMSE among the rates considered in Figure 8. We limit ourselves to lowest sampling rate of 500 Hz although we could decrease the sampling rate to the Nyquist rate of 200 Hz that is twice the maximum Doppler frequency. In practice, interpolation [11-13] and adaptive tracking accuracy [14,15] benefit from a higher sampling rate. These considerations need to be taken into account in selecting the optimal sampling rate.

Both Figures 7 and 8 illustrate the fact that the advantages of using longer memory in the prediction are more pronounced for smaller values of N. For a given model order p and sampling rate, the total memory span is given by p/f_s. For a fixed p, lower f_s implies longer memory. Thus, as f_s decreases, greater utilization of the sidelobes of the autocorrelation function becomes possible. Since the sidelobes are larger for smaller values of N, lower MMSE results when f_s is low and p is sufficiently large as N decreases. On the other hand, as f_s increases for fixed p, the prediction MMSE for any N converges to the MMSE of the Rayleigh fading. This is due to the reduction of the memory span of the prediction to the region where the autocorrelation functions are similar for all N (Fig. 6). Similarly, for low model order p, the advantage in the MMSE due to the lower number of oscillators diminishes. When short range prediction or channel estimation is the objective, short memory span is sufficient to generate reliable estimates [9,10]. Thus, the MMSE in this case is not sensitive to the number of oscillators.

3. PREDICTION IMPROVEMENT THROUGH ADAPTATION

In section 2, it was shown that long range channel prediction benefits from choosing lower sampling rate f_s given model order p. When received samples are corrupted by noise, prediction accuracy greatly decreases (see Figures 4,5 and 7). In this case, noisy received signals sampled at the high data rate (see, e.g. (2)) can be used to reduce the noise effect in the prediction, even if lower sampling rate is employed in the autoregressive filter. As new received signals y_k (2) become available, we utilize them to update previously predicted channel values $\hat{c}_n$ and model coefficients d_j. This update results in improved future predictions. Here we discuss and compare three approaches to using received signal to improve prediction accuracy. In the following discussion, we assume that the sampling rate f_s is 500 Hz, the data rate is 25 Kbits/second and f_{dm}=100Hz. Thus, there are 49 data bits between the two adjacent low rate samples. Since we often refer to two different rates in this paper, we use the index k for the samples at the data rate, and index n for the lower sampling rate throughout. We utilize channel inversion with threshold ρ [7,8,13,17], and assume the average transmitter power is normalized to 1. When the predicted channel coefficient $\hat{c}_k$ is above the threshold ρ, the received signal is given by:

$$y_k = \beta \frac{c_k}{\hat{c}_k} b_k + z_k \qquad (10)$$

where the factor $\beta = \sqrt{\frac{1}{E\left(\frac{1}{|\hat{c}_k|^2} \mid \frac{1}{|\hat{c}_k|^2} < \frac{1}{\rho}\right)}}$ is introduced here for consistence in SNR calculation [7]. The prediction accuracy factor is defined as

$$a_k = \frac{c_k}{\hat{c}_k} \qquad (11)$$

and the average SNR at the receiver is $\bar{\gamma} = \frac{\beta^2}{N_0}$. In defining the SNR, it is assumed that $E[b_k^2]=1$ and $a_k=1$. In the numerical results below we assume the threshold $\rho = 0.1$.

Initially, suppose b_k is known. Given b_k=1, the noisy estimates of channel coefficients at the *data rate* can be obtained from equation (10) as:

$$c'_k = \frac{y_k}{\beta}\hat{c}_k = c_k + \frac{\hat{c}_k}{\beta} z_k \qquad (12)$$

The SNR of these noisy samples is $\bar{\gamma}$. Similarly, the noisy channel samples at the *lower sampling rate* are given by:

$$c'_n = \frac{y_n}{\beta}\hat{c}_n = c_n + \frac{\hat{c}_n}{\beta} z_n \qquad (13)$$

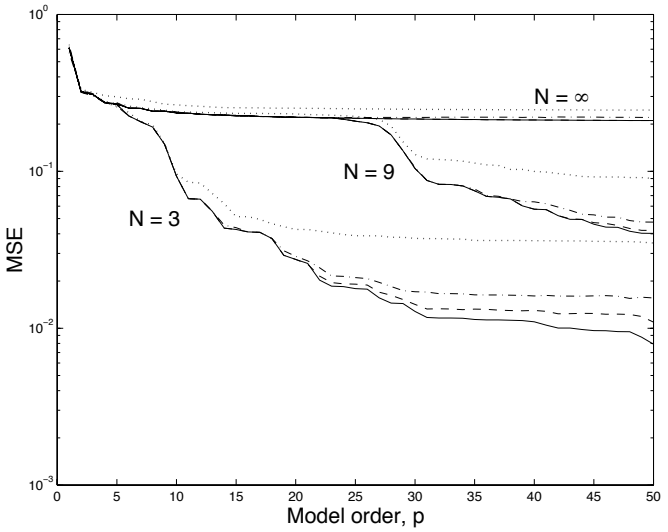

Figure 7. Theoretical MMSE vs model order, p, for Rayleigh fading (N=∞) and N=3 and 9 (solid lines) at SNR = 11.9 dB for prediction range of 2ms, f_{dm}=100Hz. Also, for each N, simulated average MSE for various observation intervals: 200 samples (…..), 1000 samples (-.-.-), and 2000 samples (- - -).

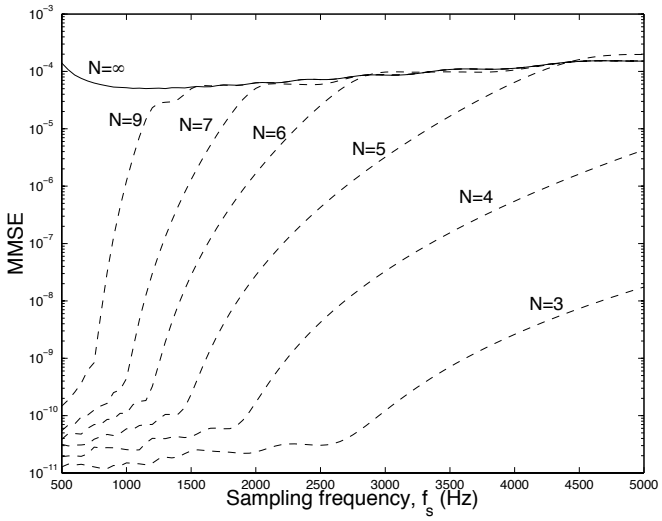

Figure 8. MMSE vs f_s for different values of N and for prediction range of 4ms, f_{dm}=100Hz at SNR=100 dB and p=50.

and the SNR of c'_n is still $\bar{\gamma}$. Now, we describe the following three approaches to using c'_k, a_k and c'_n, respectively, in the channel prediction.

(1)Wiener filtering. For this ideal case, assume that the autocorrelation function of the fading channel is known. Then the MMSE estimate of the channel coefficient c_n (at the lower sampling rate) using Wiener filtering based on 50 previous noisy samples c'_k from (12) (at the data rate) results in the minimum mean squared estimation error ξ_{min}. (We use the autocorrelation function (4) to compute ξ_{min}). This error can be viewed as the variance of the effective noise added to the actual channel sample to obtain the estimate. Then, the effective SNR for the estimated channel samples is given by $E[|c_n|^2 \mid |c_n|^2 > \rho]/2\xi_{min} = (1+\rho)/2\xi_{min}$. This effective SNR is shown by solid curve in Fig. 9 and can be viewed as an upper bound on the SNR enhancement in the low rate samples using received signal sampled at the data rate.

(2) Adaptive tracking of factor a_k. The factor a_k (11) can be adaptively updated at the data rate [17] using, e.g. Least Mean Squares (LMS) algorithm:

$$\tilde{a}_{k+1} = \tilde{a}_k + \mu e_k \hat{b}_k^* \qquad (14)$$

where μ is the step-size controlling the convergence rate. In this paper, μ is fixed at 0.1. Further prediction performance improvement can be obtained by choosing the optimal μ for each SNR value. The algorithm is decision-directed: $\hat{b}_k$ is the decision of b_k, but in this paper we assume perfect detection and set $\hat{b}_k = b_k$. The error signal e_k is defined as: $e_k = y_k - \tilde{y}_k = y_k - \beta\tilde{a}_k\hat{b}_k$. Note that error signal e_k approaches the value of the additive noise z_k when the factor $\tilde{a}_k$ is close to the actual a_k. Since the value of μ is small, the effect of noise z_k in tracking the factor a_k is not significant and the procedure of adaptive tracking of the factor a_k can be viewed as noise filtering (of course it is also useful for coherent detection of the data). The updated factor $\tilde{a}_k$ is sent back to transmitter at the lower sampling rate and used to update previously predicted fading channel coefficient $\hat{c}_n$ as $\tilde{c}_n = \tilde{a}_n\hat{c}_n$. This updated coefficient is used in the AR filtering to improve future predictions.

The effective SNR for $\tilde{c}_n$ is examined through simulation. We use the number of scatterers N=9, the observation interval of 100 samples, very low noise during the intitial observation interval, and model order p=60. The prediction range is 2ms, and the SNR is computed using 50 low rate samples following the initial observation interval. Here we just consider the updated channel coefficient $\tilde{c}_n$ in the calculation of SNR, corresponding to the part of the channel above the threshold. The SNR is shown as dotted line (circles) in Figure 9 and the corresponding prediction MSE is shown in Figure 10. The performance of this method is very good for low-to-moderate SNR, but the effective SNR and the MMSE saturate for high SNR. In practice, one will have to take into account the effect of interrupted transmission (when the channel power is below the threshold) on the performance of the adaptive algorithm and the issues associated with the decision-directed tracking (e.g., phase ambiguity, propagation error, etc).

(3) Prediction using noisy samples. The third approach is to use the estimate of c'_n (13) from the noisy received signal. The ideal SNR for this approach is given by $\bar{\gamma} = \frac{\beta^2}{N_0}$ and is shown for reference as the solid line(stars) in Figure 9. The measured SNR (from simulations) is lower due to prediction error and is shown as the dotted line (stars) in the same figure. This approach gives poor prediction performance for moderate SNR, and the performance degrades significantly when the SNR is less than 10 dB due to the noise enhancement resulting from unacceptable prediction. The comparison of the MSE for the second and third methods is shown in Figure 10.

In this paper, we assumed that parameters associated with the scatterers in equation (3) (the number N, the Doppler frequency shifts f_n, the amplitudes A_n and the phases ϕ_n) are constant during a data block. These parameters determine the choice of the LP coefficients d_j. In general, the constant parameter assumption is not strictly true [14,15] and causes parameter mismatch when fixed LP coefficients are used during the transmission interval. In addition, the short observation interval and the additive noise results in suboptimal d_j and significantly affect prediction accuracy. Adaptive update of model parameters using the LMS algorithm was proposed in [17]. Consider the following

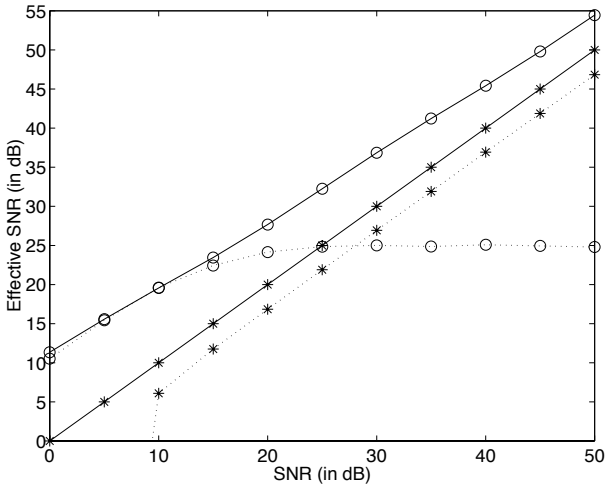

Figure 9. Effective SNR comparison for different prediction approaches. o------o: Wiener filtering; o……o: adaptive tracking of factor a_k; *------*: ideal SNR using noisy samples; *……*: measured SNR using noisy samples; prediction range of 2 ms, f_{dm}=100Hz.

equation of the adaptive update of the LP coefficients (at the low rate):

$$\underline{d}(n+1) = \underline{d}(n) + \eta e_n \underline{c}_n^* \qquad (15)$$

where η is the step-size, $\underline{d}(n)=(d_1(n), \ldots d_p(n))$ is the time-dependent vector of channel model parameters (see (3)), $\underline{c}(n) = (c_{n-1}, \ldots, c_{n-p})$ is the vector of observed channel samples and $e_n = c_n - \hat{c}_n$. Since we are interested in the MMSE of this method as a function of the SNR, we modify the definition of $\underline{c}(n)$ in (15) to represent noisy observations (as y_n in (2) with b_k=1). Joint adaptive tracking of d_j and the prediction accuracy factor a_k in the channel inversion with threshold algorithm (or another noise reduction method) could reduce the effect of the noise significantly. However, we use noisy samples here for consistency with the theoretical results in Section 2. The steady-state MMSE J_{ada} of linear prediction through adaptive tracking d_j is given by [18]:

$$J_{ada} = J_{min} + \frac{1}{2}\eta J_{min} p(1+\frac{1}{2}N_0) \qquad (16)$$

where J_{min} is the optimal MMSE of linear prediction given model order p calculated according to equation (7) assuming the autocorrelation function (4). The J_{ada} versus model order p for different SNR and η=0.015 (which was also used in [17]) is illustrated in Figure 5 (dotted lines). Simulation results in [15, 17] show that predicted values using adaptive tracking follow very closely the actual channel envelope for typical fading conditions. Also, our results show that greater prediction range than used in the simulations of this section can be afforded without significantly degrading performance.

4. Conclusion and Future Work

We discussed the advantages of using low sampling rate to achieve long range prediction and the benefits of combining prediction with adaptive tracking. Current and future work in this area focuses on practical issues associated with adaptive tracking for realistic channel models and measured data [14,15], prediction for multipath fading channels and antenna diversity systems [15,19], adaptive modulation and coding aided by long range prediction and channel estimation and equalization combined with the proposed prediction algorithm.

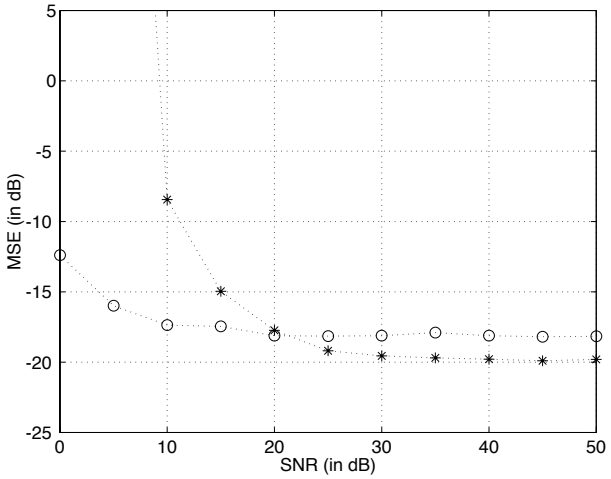

Figure 10. MSE performance comparison: o……o: adaptive tracking of factor a_k; *……*: using noisy samples.

Acknowledgment

The authors are grateful to Dr. Jack Holtzman for his helpful suggestions.

References

[1] W. C. Jakes, *Microwave Mobile Communications*, IEEE Press, 1993.

[2] J. G. Proakis, *Digital Communications*, McGraw-Hill, New York, 1995.

[3] T. S. Rappaport, *Wireless Communications*, Prentice Hall, NJ, 1996.

[4]T. Ue, S. Sampei, N. Morihiko, and K. Hamaguchi, "Symbol Rate and Modulation Level–Controlled Adaptive Modulation/TDMA/TDD System for High–Bit–Rate Wireless Data Transmission," *IEEE Trans. on Vehicular Techn.*, Vol. 47, No. 4, pp. 1134 – 1147, Nov. 1998.

[5] A. J. Goldsmith and S. G. Chua, "Adaptive Coded Modulation for Fading Channels", *IEEE Trans. on Comm.*, vol. 46, No. 5, pp. 595 - 601, May 1998.

[6] D. L. Goeckel, "Adaptive Coding for Fading Channels using Outdated Channel Estimates", Proceedings of VTC, May 1998.

[7] E. Biglieri, G. Cairo, and G. Taricco, "Coding and Modulation under Power Constraints", *IEEE Personal Communications*, pp. 32-39, June 1998.

[8] A. J. Goldsmith and S. G. Chua, "Variable-Rate Variable-power MQAM for Fading Channels", *IEEE Trans. Comm.* , vol. 45, No. 10, pp. 1218 - 1230, Oct. 1997.

[9] R. Haeb and H. Meyr, "A Systematic Approach to Carrier Recovery and Detection of Digitally Phase Modulated Signals on Fading Channels", *IEEE Transactions on Comm.*, 37(7): 748-754, July 1989.

[10]Y. Liu and S. D. Blostein, "Identification of Frequency Non selective Fading Channels Using Decision Feedback and Adaptive Linear Prediction," *IEEE Trans. on Commun.*, Vol. 43, No. 2/3/4, pp. 1494 – 1492, Feb./March/April 1995.

[11] T. Eyceoz, A. Duel-Hallen, and H. Hallen, "Prediction of Fast Fading Parameters by Resolving the Interference Pattern", *Proc. of the 31st ASILOMAR Conf. on Signals, Systems, and Computers*, pp. 167 – 171, 1997.

[12] T. Eyceoz, A. Duel-Hallen, and H. Hallen, "Using the Physics of the Fast Fading to Improve Performance for Mobile Radio Channels", in *Proc. 1998 IEEE International Symposium on Information Theory*, p.159.

[13] T. Eyceoz, A. Duel-Hallen, and H. Hallen, "Deterministic Channel Modeling and Long Range Prediction of Fast Fading Mobile radio Channels", *IEEE Comm. Letters*, Vol. 2, No. 9, pp. 254 – 256, Sept. 1998.

[14] H. Hallen, S. Hu and A. Duel-Hallen, "Physical Insights into the Nature of the Fast Fading in Wireless Communications", *to be submitted to JSAC.*

[15] S. Hu, H. Hallen and A. Duel-Hallen, "Physical Channel Modeling, Adaptive Prediction and Transmitter Diversity for Flat Fading Mobile Channels," Proceedings of SPAWC'99.

[16] J. K. Cavers, "An Analysis of Pilot Symbol Assisted Modulation for Rayleigh Fading Channels", *IEEE Trans. on Vehicular Techn.*, Vol. 40, No. 4, pp. 686 – 693, Nov. 1991.

[17] T. Eyceoz, S. Hu, A. Duel-Hallen, and H. Hallen "Adaptive Prediction, Tracking and Power Adjustment for Frequency Non-Selective Fast Fading Channels", to appear in Proc. of the *Eighth Communication Theory Mini Conference (CTMC'99, ICC'99)*.

[18] S. Haykin, *Adaptive Filter Theory*, Prentice Hall, 1991.

[19] T. Eyceoz, S. Hu, A. Duel-Hallen, and H. Hallen "Transmitter Antenna Diversity and Adaptive Signaling Using Long Range Prediction for

Fast Fading DS/CDMA Mobile Radio Channels", to appear in *Proc. IEEE Wireless Communications and Networking Conference (WCNC'99).*